Published in final edited form as:
Connect Tissue Res. 2013 ; 54(3): 187–196. doi:10.3109/03008207.2013.778839.

Engineering and Characterization of the Chimeric Antibody that Targets the C-terminal Telopeptide of the α2 Chain of Human Collagen I: A Next Step in the Quest to Reduce Localized Fibrosis

Jolanta Fertala[1], **Andrzej Steplewski**[1], **James Kostas**[1], **Pedro Beredjiklian**[2], **Gerard Williams**[2], **William Arnold**[2], **Joseph Abboud**[2], **Anshul Bhardwaj**[3], **Cheryl Hou**[1], and **Andrzej Fertala**[1,*]

[1]Department of Orthopaedic Surgery, Jefferson Medical College, Thomas Jefferson University, Philadelphia, Pennsylvania, U.S.A

[2]Department of Orthopaedic Surgery, Rothman Institute, Thomas Jefferson University, Philadelphia, Pennsylvania, U.S.A

[3]Department of Biochemistry and Molecular Biology, Kimmel Cancer Center, Thomas Jefferson University, Philadelphia, Pennsylvania, U.S.A

Abstract

Inhibition of the extracellular process of collagen fibril formation represents a new approach to limiting posttraumatic or postsurgical localized fibrosis. It has been demonstrated that employing a monoclonal antibody that targets the C-terminal telopeptide of the α2 chain of collagen I blocks critical collagen I-collagen I interaction, thereby reducing the amount of collagen deposits *in vitro* and in animal models. Here, we developed a chimeric variant of a prototypic inhibitory antibody of mouse origin. The structure of this novel antibody was analyzed by biochemical and biophysical methods. Moreover, detailed biochemical and biological studies were employed to test its antigen-binding characteristics. The ability of the chimeric variant to block formation of collagen fibrils was tested *in vitro* and in high-density cultures representing fibrotic processes occurring in the skin, tendon, joint capsule, and gingiva. The potential toxicity of the novel chimeric antibody was analyzed through its impact on the viability and proliferation of various cells and by testing its tissue cross-reactivity in sets of arrays of human and mouse tissues. Results of the presented studies indicate that engineered antibody-based blocker of localized fibrosis is characterized by the following: (i) a correct IgG-like structure, (ii) a high-affinity and high-specificity for a defined epitope, (iii) a great potential to limit accumulation of collagen-rich deposits, and (iv) a lack of cytotoxicity and non-specific tissue reactivity. Together, the presented study shows the great potential of the novel chimeric antibody to limit localized fibrosis, thereby setting ground for critical preclinical tests in a relevant animal model.

Keywords

localized fibrosis; chimeric antibody; collagen fibrils; extracellular matrix; therapeutic antibody; protein engineering

*Correspondence to Andrzej Fertala, Department of Orthopaedic Surgery, Jefferson Medical College, Thomas Jefferson University, Curtis Building, Room 501, 1015 Walnut Street, Philadelphia, PA 19107, U.S.A. Tel: 215-503-0113, andrzej.fertala@jefferson.edu.

DECLARATION OF INTEREST

The authors report no conflicts of interest. The authors alone are responsible for the content and writing of this article.

INTRODUCTION

The potential formation of human anti-mouse antibodies (HAMA) limits the clinical utility of the mouse-derived monoclonal antibodies developed against a specific therapeutic target. Because of this limitation, various techniques have to be employed to minimize the HAMA response. For example, protein engineering approaches are utilized to reduce the content of mouse-derived antibody fragments. These approaches include (i) engineering chimeric antibodies consisting of mouse-derived variable regions fused with the human-derived constant regions, (ii) production of humanized antibodies in which the majority of variable regions and the entire constant regions are of human origin, and (iii) creation of single chain variable fragments (scFv) in which the constant regions of the native antibody are removed and the variable regions are connected via a short peptide-linker [1–6].

In this study, we focused on developing a clinically-relevant chimeric antibody variant designed to inhibit excessive accumulation of collagen-rich fibrotic deposits via blocking collagen-collagen interactions critical for the formation of collagen fibrils, a main component of fibrotic tissues [7]. Previously, we demonstrated that the mouse monoclonal antibody which targets the C-terminal telopeptide of the α2 chain (α2Ct) of the human procollagen I (anti-α2Ct) is effective in blocking collagen fibril formation *in vitro* and in keloid-like constructs [7]. Because of its mouse origin, this archetypical mouse antibody of the IgA type, however, cannot be considered an acceptable candidate for human-relevant tests. Consequently, we engineered a chimeric antibody variant (^{ch}IgG) consisting of the variable domains derived from the prototypic IgA-type anti-α2Ct antibody and the constant domains of the human IgG (^{h}IgG). Detailed analyses of the recombinant ^{ch}IgG variant demonstrated its correct structure. Moreover, this novel antibody was also tested for its ability to inhibit collagen fibril formation *in vivo* and in cultures of various cells associated with the fibrotic process. Results demonstrate a great potential of the ^{ch}IgG variant for preclinical tests with the use of relevant biological models.

MATERIALS AND METHODS

Amplification of DNA sequence encoding the V_H region of the mouse α chain (mV_H)

Total RNA was isolated from mouse-derived hybridoma cells producing the original anti-α2Ct antibody of the IgA (^{m}IgA) class [7]. Subsequently, hybridoma-derived RNA was employed as a template to generate a PCR product spanning the sequence encoding the mV_H region of the α chain of the ^{m}IgA antibody (Fig. 1). The Ig-Primer Sets (EMD Millipore/Novagen) were employed to target the 5′ end of the sequence of interest while the 3′ end was targeted with custom-designed primers (Table I) [8].

Amplification of DNA sequence encoding the V_L region of the mouse κ chain (mV_L)

A commercial Ig-Primer Set (EMD Millipore/Novagen) was employed to generate a PCR product corresponding to the mV_L of the κ chain.

Cloning the PCR fragments

The PCR products for the mV_H and the mV_L regions were cloned into the pETBlue-1 Perfectly Blunt vector (EMD Millipore/Novagen).

DNA constructs for the chimeric mV_H-human γ chain (mV_H-hγ)

To facilitate cloning into the pFUSE-CHIg-hG1 vector that includes the sequence encoding the constant region of the heavy γ chain of the human IgG_1 and the Zeocin-resistance gene (InvivoGen), the *EcoRI* and *NheI* restriction sites were introduced via PCR to the original DNA sequence encoding the mV_H region. Subsequently, an insert encoding the mV_H region

of the mouse α chain was cloned into the corresponding restriction sites of the pFUSE-CHIg-hG1 vector. The fidelity of the mV_H-hγ construct was confirmed by DNA sequencing.

DNA constructs for chimeric mV_L-human light κ chain (mV_L-hκ)

To enable cloning into the pFUSE2-CLIg-hk vector that includes the sequence encoding the constant region of the human light κ chain and the Blasticidin-resistance gene (InvivoGen), the *AgeI* and *BsiWI* restriction sites were introduced via PCR to the original DNA sequence encoding the mV_L region of the light κ chain. Subsequently, the insert encoding the mV_L region was cloned into the corresponding restriction sites of the pFUSE2-CLIg-hk vector. The fidelity of the mV_L-hκ construct was confirmed by DNA sequencing.

Selection of clones co-expressing chimeric mV_H-hγ and mV_L-hκ variants in mammalian cells

Chinese Hamster Ovary cells (CHO; ATTC# CCL-61) were transfected with DNA constructs encoding the mV_H-hγ and mV_L-hκ variants. Subsequently, Zeocin and Blasticidin-resistant clones were selected and screened for the presence of the mV_H-hγ and mV_L-hκ chains by Western blot. For these assays the goat anti-human γ chain antibodies and goat anti-human κ chain antibodies conjugated with HRP were employed (Sigma-Aldrich).

Purification of the ^{ch}IgG consisting of the mV_H-hγ and mV_L-hκ chains

Selected CHO clones were cultured in serum-free conditions in the FiberCell System (FiberCell Systems Inc.). The ^{ch}IgG was purified by affinity chromatography using Protein-L agarose, a resin that specifically binds to the light κ chain (Thermo Scientific). The molecular mass of purified ^{ch}IgG, was analyzed by size-exclusion chromatography (SEC) using the BioBasic SEC-300 column (Thermo Scientific). For these assays, ^{ch}IgG concentrated to 20 mg/ml was injected to the column equilibrated with PBS. Subsequently, the mass of protein eluted in a single peak was calculated based on the elution profiles of protein mass markers (Sigma-Aldrich).

Structural assays of the ^{ch}IgG

Circular dichroism (CD) spectra in the far-UV region were recorded for the inhibitory ^{ch}IgG variant and non-inhibitory control ^{h}IgG (Bethyl Laboratories) using the Jasco J-810 spectropolarimeter equipped with a thermostated cell holder and interfaced with a Peltier temperature controller (Jasco Products Co.). Scans were performed at 4°C with 2 μM final protein concentration. The molar mean residue ellipticity [θ] in deg cm^2 $dmol^{-1}$ was obtained from the measured raw data after subtracting the buffer spectrum, taking into account the measured ellipticity in millidegrees (θ), the molar protein concentration in mol/l (c), the optical pathlength in cm (l), the number of amino acid residues (N) (1364 residues), and molecular mass (Mw) (150 kDa) according to the relation:[θ]/θ/(10.c.l). A mean residue molecular mass of 109.97 Da was used for both samples. Typically, CD spectra were measured in the wavelength range of 200–260 nm, and rectangular quartz cuvette with a path length of 0.1 cm was used. Low-noise circular dichroism spectra were measured by averaging five scans. Data were collected at 0.5-nm intervals using a bandwidth of 2 nm, response time of 1 s and averaging time of 30 s for each measurement. Secondary structure contents were calculated by the K2d method available on the DichroWeb Server [9].

Generation of the $F(ab')_2$ fragment of the ^{ch}IgG

The $F(ab')_2$ fragment (Fig. 1) was generated by cleaving the purified ^{ch}IgG variant with IdeS, a cysteine proteinase secreted by the *Streptococcus pyogenes* which specifically cleaves the heavy chain of IgG (FabRICATOR, Genovis AB) [10, 11].

Western blot assays of antigen specificity of intact ^{ch}IgG and its F(ab′)$_2$ fragment

To detect the binding of the intact ^{ch}IgG to the pro-α2 chain target electroblotted onto a nitrocellulose membrane, the anti-human γ-chain antibodies conjugated with HRP were employed. In similar assays, the binding of the F(ab′)$_2$ fragment was detected with the HRP-conjugated anti-human κ chain antibodies (Sigma-Aldrich). Following Western blots, procollagen and procollagen-derived bands were visualized with the Ponceau S by the direct staining of nitrocellulose membranes. Such staining was helpful in precisely determining the patterns of electrophoretic migration of analyzed protein bands.

Biosensor-based binding assays

The ability of the prototypic ^{m}IgA anti-α2Ct antibody to specifically bind the-α2Ct in both procollagen I and collagen I has been previously demonstrated [7]. Here, binding interactions between intact procollagen I and the ^{m}IgA, the ^{ch}IgG or the F(ab′)$_2$ variants were studied with the use of the SensiQ Pioneer biosensor (SensiQ Technologies Inc.). In addition, binding interactions of control human IgG and control mouse IgA were also studied. In brief, procollagen I was immobilized on a sensor, as described [12, 13]. Following procollagen immobilization, free antibody variants solubilized in HEPES-buffered saline (HBS, 10 mM HEPES, 150 mM NaCl, and 0.005% Tween 20, pH 7.4) were injected in separate cycles at concentrations ranging from 12.5 to 200 nM. After collecting data representing the association phase, antibody-free HBS was injected to the sensor, and the dissociation phase was recorded. After each assay, the surface of the sensor was regenerated by washing with 10 mM HCl, followed by equilibration with HBS. Data from the biosensor were analyzed by the global fitting method with the use of the QDat software (SensiQ Technologies Inc.) [14]. For each assay, the association rate constants (k_{on}) and the dissociation rate constants (k_{off}) were obtained, and the equilibrium dissociation constants (K_D) values were calculated from the k_{off}/k_{on} ratios.

Inhibition of collagen fibril formation *in vitro*

The potential of the ^{ch}IgG variant of the anti-α2Ct antibody to block formation of collagen fibrils *in vitro* was examined, as described [7]. In brief, the ^{m}IgA or ^{ch}IgG variant of the anti-α2Ct antibody was added to the collagen I samples at 1:1 collagen: antibody molar ratio. Subsequently, collagen fibril formation was triggered by incubating the samples at 37°C. Next, at predefined time points, the samples were centrifuged to separate collagen fibrils (pellet fractions) from collagen I monomers (supernate fractions). Later, the pellet and the supernate fractions were analysed by gel electrophoresis. Samples without antibodies and those containing ^{h}IgG isolated from normal human serum were employed as controls. Note that collagen fibrils formed using this method have chracteristics of native fibrils preserved and retain epitopes recognized by studied anti-α2Ct antibodies [7]. Still, proper assembly of fibrils formed in control groups was monitored by transmission electron microscopy, as described [7]. In brief, 10-μl samples containing fibrils formed for 24 h were transferred onto 200-mesh Formvar-supported and carbon-coated copper grids (Ted Pella, Inc.). Collagen fibrils deposited on the grids were stained negatively with 1% phosphotungstate (pH 7.0) and visualized by a transmission electron microscope operating at 75 kV (model H-7000, Hitachi Ltd.).

Inhibition of formation of collagen deposits in layers of cells cultured in the presence of the anti-α2Ct ^{ch}IgG

Note: patient-derived primary cells were collected from discarded tissues with the permission of the Institutional Review Boards of the participating institutions.

Assays of inhibition of collagen fibril deposition were done in cultures of dermal fibroblasts, keloid-derived fibroblasts, tenocytes, cells from the shoulder capsule derived from a patient with adhesive capsulitis, cells isolated from the tissue associated with the palmar fibromatosis, and in cultures of gingival fibroblasts isolated from patients diagnosed with gingival fibromatosis. In brief, for the Western blot assays, 5×10^4 cells were seeded into a 24-well plate, while for the immunostaining assays, 1.5×10^4 cells were seeded into wells of an 8-well slide. The ^{ch}IgG was added to the medium at a concentration of 70 μg/ml and the medium was changed every 2 days. Control groups consisting of cells treated with ^{h}IgG and non-treated cells were also prepared.

For the Western blot assays, cell layers were lysed and then proteins were analyzed; collagen I was detected with the use of polyclonal anti-collagen I antibodies (AFCol-1) prepared for us by Abgent Inc. while glyceraldehyde 3-phosphate dehydrogenase (GAPDH) was detected with the anti-GAPDH antibody (Santa Cruz Biotechnology Inc.).

For immunostaining assays, the cell layers were fixed with methanol and then collagen fibrils were stained with the primary AFCol-1 rabbit anti-collagen I antibodies and the secondary anti-rabbit-IgG antibodies conjugated to the Alexa Fluor 594 (Invitrogen). Nuclei were visualized with 4′,6-diamidino-2-phenylindole (DAPI) staining. Immunostained cell layers were observed with a fluorescence microscope (Eclipse E600, Nikon Inc.).

Cytotoxicity assays

Cytotoxicity assays for the ^{ch}IgG were carried out with human dermal fibroblasts and with cells isolated from the human tendon sheath. These assays were done with the use of the WST-8 compound whose cell-mediated catabolism is observed colorimetrically (Sigma-Aldrich). First, the ability of the selected assay to detect changes in the viability of cells in response to a cytotoxic agent was experimentally tested. In brief, fibroblasts seeded in Dulbecco's Modified Eagle's Medium (DMEM) supplemented with 10% fetal bovine serum (FBS) at a density of 10,000 cells/microplate-well were treated with increasing concentrations of tissue necrosis factor α (TNFα) for 24 h in the presence of 1.0 μg/ml of actinomycin-D (Sigma-Aldrich). After that time, the changes in response to a varying amount of TNFα were recorded. Next, the potential of the anti-α2Ct antibody to induce the acute cytotoxicity was analyzed by measuring the viability of cells treated for 24 h with increasing concentrations, up to 200 μg/ml, of the tested antibody variants. Control groups treated with ^{h}IgG and PBS only were also employed. In these assays, data were presented by employing a linear fit (GraphPad Prism software, GraphPad Software Inc.)

The possible toxicity of the ^{ch}IgG was also tested by analyzing its impact on cell proliferation. In brief, analyzed cells were cultured for 6 days in DMEM supplemented with 10% FBS in the presence of the ^{ch}IgG added to the media at a concentration of 100 μg/ml. At the specific time intervals, the relative amounts of the metabolic product of WST-8 catabolism were assayed colorimetrically. Employing control groups consisting of cells cultured in the presence of 2 ng/ml of pro-proliferative platelet-derived growth factor (PDGF; Sigma-Aldrich), and those cultured in the presence of 1.0 μg/ml of anti-proliferative actinomycin-D, validated the described test. Additional control groups included cells treated with ^{h}IgG and PBS only. In these assays, data were presented by employing an exponential fit (GraphPad Prism software, GraphPad Software Inc.)

Cross-reactivity assays

To analyze the possible cross-reactivity of the anti-α2Ct antibody, we employed a Food and Drug Administration-recommended method in which the tissue cross-reactivity of a tested agent is analyzed by immunohistology done on arrays of various tissues. The cross-

reactivity assays in human tissues (USBiomax, Inc.) were carried out with the use of the original ^{m}IgA variant of the anti-α2Ct antibody, whose antigen specificity is identical to that of its ^{ch}IgG counterpart [7]. For these assays, biotinylated rat anti-mouse-IgA antibodies were used as the secondary antibodies (eBioscience). The cross-reactivity of the ^{ch}IgG variant was analyzed with the use of the mouse-derived tissue arrays (US Biomax, Inc.). For these assays, biotinylated goat anti-human-IgG antibodies were employed as the secondary antibodies (Vector Laboratories, Inc.). Following immunostaining, all samples were counterstained with Methyl Green (Vector Laboratories, Inc.). Moreover, the general morphology of the analyzed tissues was observed after staining corresponding samples with hematoxylin and eosin.

RESULTS

PCR products encompassing DNA sequences for the mV_H and the mV_L of the prototypic ^{m}IgA-type anti-α2Ct antibody

Based on the PCR results, a set of primers including MuIgV_H5′-C and α1_1 primers (Table I) was selected to generate DNA fragment encoding the mV_H (Fig. 1). The forward MuIg$_κV_L$5′-G and the reverse MuIg$_κV_L$3′-1 primers were selected to generate a DNA fragment encompassing the sequence for the mV_L of the mouse light κ chain (Fig. 1 and Table I).

Composition and binding-specificity of the intact ^{ch}IgG

The specific chain composition of purified ^{ch}IgG was confirmed by Western blot (Fig. 2A and 2B). A distinct protein band seen after electrophoresis of the purified ^{ch}IgG in non-reducing conditions indicates that this variant produced by CHO cells forms a disulfide bond-stabilized mV_H-hγ/mV_H-hκ complex (Fig. 2B). As depicted in Fig. 2C, the anti-α2Ct ^{ch}IgG antibody specifically recognized only the pro-α2 chain and a product of its partial processing, both including the α2Ct epitope. In contrast, no pro-α1 chain was detected, thereby indicating the high specificity of this anti-α2Ct variant.

F(ab′)$_2$ fragments

Treatment of the recombinant ^{ch}IgG with IdeS that specifically cleaves IgG at a site present within its hinge region has generated fragments of the predicted molecular masses (Fig. 2D). Specifically, in the non-reducing electrophoretic conditions the IdeS-generated products were apparent as a 100 kDa band corresponding to the F(ab′)$_2$ fragment and a band representing the Fc fragment migrating in the range of 27 kDa (Fig. 2D). As demonstrated in Fig. 2E, the F(ab′)$_2$ fragment specifically recognizes the pro-α2 chain and a product of its partial processing, both including the α2Ct epitope. Similar to the intact ^{ch}IgG, no pro-α1 chain was detected, thereby indicating an epitope specificity of the F(ab′)$_2$ fragment. Individual lanes seen in Fig. 4E represent samples loaded at increasing concentrations.

Structural characteristics of the ^{ch}IgG

Essential structural characteristics of the ^{ch}IgG were analyzed with the use of CD spectroscopy. Analysis of data from the CD assays (Fig. 3A) demonstrated that α-helices, β-sheets, and random-coil conformations contribute 3%, 50%, and 47%, respectively, to the structure of control ^{h}IgG. The corresponding values for the inhibitory ^{ch}IgG variant were 7%, 45%, and 48%, thereby further indicating the native-like structure of the therapeutic ^{ch}IgG antibody. In addition, the SEC assays (Fig. 3B) have determined that 100% of the ^{ch}IgG variant was produced by CHO cells in a monomeric form of the expected molecular mass of 150 kDa.

Biosensor binding assays

As indicated in Fig. 4, the ^{m}IgA-procollagen I binding is characterized by the equilibrium dissociation constants (K_D) of 0.2 nM, while the corresponding value for the ^{ch}IgG-procollagen I and F(ab′)$_2$-procollagen I binding is 3.2 nM and 2.8 nM, respectively. The lack of binding of the control mouse IgA (not shown) and control ^{h}IgG to procollagen I further corroborate binding specificities of the analyzed anti-α2Ct variants (Fig. 4).

Inhibition of fibril formation *in vitro*

As evident by the lack of collagen in the fibril/pellet fractions, the ^{ch}IgG variant applied at a 1:1 molar ratio with procollagen I has completely blocked the fibril formation process (Fig. 5A). In applied experimental conditions, the inhibitory activity of the ^{ch}IgG was similar to that seen for the prototypic anti-α2Ct ^{m}IgA variant (Fig. 5B). In contrast, the fibril formation process was not affected in control groups prepared in the absence of the inhibitory antibodies (Fig. 5C) or in the presence of non-inhibitory ^{h}IgG (Fig. 5D). In these groups, the presence of fibrils in the pellet fractions was readily detectable, and as indicated in Fig. 5E, their overall morphology and apparent periodicity resembled that of a typical collagen fibril.

Inhibition of formation of collagen deposits in cell layers in the presence of the ^{ch}IgG variant

As indicated in Figure 6, in the presence of control ^{h}IgG, all analyzed cells deposited collagen-rich matrices around them. The gross morphologies of deposited collagen fibrils and their densities varied among analyzed cells. For instance, the apparent density of readily visible fibrils was relatively high in matrices formed by the dermal fibroblasts and tenocytes. In contrast, the apparent overall density of thin fibrils formed by cells isolated from fibrotic gingiva was relatively low. In all analyzed cell types, however, a reduction in the relative amounts of accumulated collagen-rich deposits in the presence of the ^{ch}IgG was readily visible (Fig. 6). More quantitative Western blot assays done to detect collagen I present in cell layers further demonstrate the reduction of accumulated collagen I-rich deposits in cells cultured in the presence of the ^{ch}IgG variant (Fig. 7). Specifically, densitometric assays of the fully processed α1 chain extracted from the cell layers demonstrated that in comparison to the control treated with ^{h}IgG, the reduction of deposited collagen ranged from about 60% in keloid-derived fibroblasts, tenocytes, and cells from the joint capsule to about 90% in dermal fibroblasts, cells isolated from palmar fibromatosis tissue, and gingival fibroblasts. Note, that multiple bands seen above the α1 chain of collagen I most likely represent the intermediate products of the processing of pro-α1 chain, and some of them may also represent the crosslinked forms of the α1 chain.

Effects of the ^{ch}IgG on the viability of cells

As seen in Fig. 8A, increasing the concentration of the ^{ch}IgG variant to 200 μg/ml, a 2.5-fold concentration of that employed for the cell-based inhibitory assays (Figs. 6), did not have any significant acute toxic effects on the viability of tested cells. The ability of the employed test to detect changes in the viability of cells treated with increasing concentrations of TNFα, validates its utility (Fig. 8B). The effects of the ^{ch}IgG on the viability of selected cells were also analyzed by monitoring their proliferation. As shown in Fig. 8C and 8D, the presence of tested antibodies added to the cell culture media at a concentration of 100 μg/ml did not have any effect on proliferation. The proliferation characteristics, illustrated by the fitted curves, of cells cultured in the presence of ^{ch}IgG or ^{h}IgG were similar to these observed for cells cultured in the absence of IgG variants. An accelerated proliferation of cells in the presence of PDGF and the lack of proliferation in the presence of actinomycin D validate the utility of the applied assay (Fig. 8C and 8D). Although the above proliferative behavior seen in response to various factors was similar in tested dermal fibroblasts (Fig.

8C) and cells isolated from the tendon sheaths (Fig. 8D), the specific dynamics of proliferation differed in these cell types. These differences are most likely attributed to broad biological differences expected in primary cells isolated from distant tissues.

Cross-reactivity assays

As indicated in Fig. 9A, the ^{m}IgA variant specifically recognized the collagen I-rich dermis of the human skin; in the same conditions, no staining of epidermis, a skin layer that lacks collagen I, was observed. In a similar set of experiments, the ^{ch}IgG variant was tested with the mouse-derived tissues. A positive staining of the collagen I-rich dermis and a negative result of staining of epidermis was observed (Fig. 9B). Note that in contrast to the human skin, the mouse epidermis consists only of a thin layer of keratinocytes, thereby making them less clearly visible (Fig. 9B). Moreover, in both skin samples, some nonspecific weak staining of keratinized epidermis is observed. The lack of staining of tissues in which collagen I is poorly represented was also determined. For instance, the expected positive staining of the interlobular regions of a mouse thymus was observed under a high magnification, while collagen I was not detected in the lobular regions of this tissue (Fig. 9B). Together, the cross-reactivity assays demonstrate the high specificity of the ^{m}IgA and the ^{ch}IgG variants for the binding of the collagen I target.

DISCUSSION

Excessive scar formation and fibrosis is a common clinical problem. A hallmark of such a tissue is the presence of collagen-rich deposits formed in the process that involves inflammation and activation of cells. To date, therapeutic approaches to limit fibrosis have included anti-inflammatory and anti-proliferative agents such as steroids, mitomycin C, 5-fluorouracil, among many others [15–17]. All of these approaches have been met with little clinical success [18]. Recently, our group has proposed that the extracellular process of collagen fibril formation may serve as a valid target to reduce the mass of collagen-rich fibrotic tissues [7, 19]. We postulated that targeting the specific process of fibril formation may offer not only an effective but also a safe way to reduce the growth of fibrotic tissue at the site of accidental or postoperative trauma. Since fibril formation is driven by the telopeptide-mediated collagen-collagen interaction, we generated the anti-α2Ct antibody that specifically binds to the telopeptide of the α2 chain of human collagen I, thereby blocking its critical binding interactions [7, 19–21]. Consequently, the anti-α2Ct antibody was tested as the inhibitor of localized fibrosis in a keloid-like model [7]. As described by Chung *et al*., these initial tests indicated the great potential of the anti-α2Ct antibody to reduce the mass of the formed fibrotic tissue [7].

Because the prototypic anti-α2Ct antibody is of mouse origin and it belongs to the IgA class, its utility to serve as a therapeutic agent in human patients is limited [22, 23]. To circumvent this limitation, we rationally engineered the chimeric anti-α2Ct antibody variant consisting of the murine variable domains of the α and κ chains and the constant regions of the human γ and κ chains. Our proposed strategy is supported by the fact that to date a number of chimeric therapeutic antibodies exist in the market. Examples of such antibodies include Basiliximab, Cetuximab, and Infliximab [24]. Biophysical and biochemical assays of the ^{ch}IgG variant indicate its native-like structure characterized by the specific assembly of the light and heavy chains and the content of the α-chains and β-sheets similar to that of the wild type ^{h}IgG. Moreover, lack of non-specific aggregation of the ^{ch}IgG variant, demonstrated by a single chromatographic peak corresponding to the predicted molecular mass of a monomer, further indicates the proper structure of the ^{ch}IgG variant. As formation of soluble and insoluble antibody aggregates is indicative of abnormal folding of engineered antibodies, a feature that may reduce their bioactivity and increase the risk for

immunogenicity, our data indicate the promising potential of the ^{ch}IgG variant for preclinical tests in relevant biological models [25–27]. Furthermore, preservation of the therapeutic utility of the engineered ^{ch}IgG form of the anti-α2Ct antibody is indicated by the results of Western blot assays which indicate that the ^{ch}IgG variant retains its antigen specificity. Of interest is the observation that the antigen specificity has been preserved in the F(ab′)$_2$ fragment of the ^{ch}IgG. This observation is particularly critical in the context of the intended use of the ^{ch}IgG. Specifically, the proposed action of the anti-α2Ct antibody is based on its antigen-binding function rather than on the effector function. In fact, it is conceivable that the potential Fc-mediated effector function of the anti-α2Ct antibody could indeed be a limiting factor for its envisioned anti-fibrotic applications. Thus, the ability of the F(ab′)$_2$ fragment to bind the α2Ct target furthers the prospect of the anti-α2Ct antibody for being used as a safe inhibitor of the formation of fibrotic deposits.

One of the challenges in engineering of therapeutic antibodies is to maintain their high affinity for binding to the designated target. Thus, preserving the specific, high-affinity binding of an antibody is critical not only for achieving the therapeutic objective but also for reaching this objective in a safe way with the smallest possible concentration of administered antibody [5]. Analyses of the binding kinetics of the ^{ch}IgG and its F(ab′)$_2$ fragment demonstrated a nM-range of the K_D values, thereby indicating a strong binding affinity. Of note is the fact that the specific K_D values reported in the presented study were obtained with the use of intact procollagen I molecules serving as binding partners for the tested antibody variants. In our previously reported work, we suggested that a bulky C propeptide of procollagen I may partially restrict the access of the anti-telopeptide antibodies to their specific epitopes, thereby influencing the binding kinetics [7]. Consequently, we expect that the affinities of the tested anti-α2Ct variants for the binding of the α2Ct present in the fully processed collagen I may be greater than those reported for the binding interactions with intact procollagen I. Still, K_D values for the ^{ch}IgG and its F(ab′)$_2$ fragment were higher than that calculated for the original ^{m}IgA variant. Such changes in binding affinities are frequently seen in engineered antibody variants and they are explained by the differences in the primary structures of antibody variants and by changes in the posttranslational modifications such as glycosylation [5].

Similar to its original ^{m}IgA counterpart, the ^{ch}IgG version of the anti-α2Ct was also active in inhibiting collagen self-assembly *in vitro*. In addition, the efficacy of the ^{ch}IgG variant to limit the formation of collagen-rich deposits was demonstrated in cell culture conditions. Although the employed system does not fully represent the native tissues, it provides an opportunity to test the blocking potential of the analyzed antibody in a complex environment created by cultured cells. The inhibitory characteristics of the ^{ch}IgG variant seen in cultures of cells isolated from tissues such as skin, tendon, tendon sheath, and gingiva point toward the therapeutic utility of this antibody in a broad range of tissues prone to developing localized fibrotic deposits in response to trauma. The above *in vitro* and cell-based assays do not clearly answer, however, to what extent the proposed antibodies are able to reach their intended target *in vivo*. In comparison to the *in vitro* and cell-based experimental systems, the access of a 150,000-Da antibody to the sites of collagen fibril formation may be hampered by a compact structure of a targeted connective tissue. In addition, in some tissues, the access to specific target sites may be limited due to the presence of cell membrane indentations reported to serve as sites for the initial stages of procollagen processing and collagen fibril formation in a developing tendon of a chick embryo [28]. Indirect evidence for the ability of antibodies to penetrate the structure of connective tissues is provided by some pathological situations associated with the presence of auto-antibodies. For instance, in epidermolysis bullosa acquisita, a blistering disease, the formation of the anchoring fibrils is altered by the auto-antibodies that interfere with collagen VII-collagen VII interaction. Similarly, the alteration of the formation of the collagen IV network via

auto-antibodies that bind to a specific region of this collagen type is a fundamental cause of Goodpasture's syndrome.

Although the above considerations about the accessibility of target sites have to be addressed in relevant animal models, we postulate that the potential problems with the access of inhibitory antibodies to the target sites could be circumvented by, for example, optimizing the antibody-delivery methods. Moreover, engineering relatively small antibody variants, *e.g.* a 25,000-Da scFv construct, could improve their diffusion characteristics, thereby enhancing their potential therapeutic utility.

One of the critical considerations for the use of a therapeutic antibody is its potential cytotoxicity and cross-reactivity. As demonstrated by viability assays of cells treated with varying concentrations of the ^{ch}IgG, the cytotoxic effects of the tested antibody have not been observed in the applied range of antibody concentrations. Although monoclonal antibodies are developed to recognize a specific epitope, they may cross-react with different epitopes and cause toxicity [23]. To test for such a possibility, it is recommended to check the immunoreactivity of a candidate antibody in a panel of various tissues [23]. In the presented study, these tests were done with the original ^{m}IgA and the ^{ch}IgG variants with the use of human and mouse-derived tissues, respectively. Results of immunostaining assays indicate the great specificity of the tested antibody variants. Although we demonstrated the binding of inhibitory antibodies to the collagen-rich tissues, their ability to bind the established collagen fibrils *in vivo* is not currently determined. We expect, however, that binding of these antibodies to established fibrils *in vivo* is limited. Specifically, we predict that, unlike in immunohistological assays done on slices of tissues in which antibody-binding sites are exposed due to the histological processing of samples, in the native fibrils the access to the α2-Ct telopeptide may be restricted [29, 30]. Still, considering the recent report by Antipova and Orgel it is evident that anti-biglycan antibodies are able to penetrate collagen fibers and partially dissociate them by disrupting biglycan-mediated inter-fibrillar interactions [31]. Considering these recent observations, further studies are needed to clearly establish whether the anti-α2Ct antibody is able to gain the access to its telopeptide target present in the gap region of mature fibrils. Such information will be helpful to determine whether the proposed antibody is only able to block the formation of newly created fibrils or whether it is also capable of decomposing already-formed fibrotic deposits.

The described study presents a critical step in a quest to implement a novel approach to inhibit localized fibrotic responses via blocking the formation of the collagen-rich deposits, namely by developing a therapeutically-relevant form of the anti-α2Ct antibody [7]. Overall, the presented study demonstrates the great potential of the bioengineered ^{ch}IgG variant of the anti-α2Ct antibody to be considered for preclinical tests in a relevant animal model. The most prominent characteristics that support this notion include a proper antibody structure, a high antigen specificity, a high antigen-binding affinity, and a low risk for toxicity. Planned future studies will provide critical preclinical data that will help to determine the prospects and limits of the proposed approach to limit localized fibrosis in injured connective tissues.

Acknowledgments

This work was supported by grants from NIH to A.F. (AR061118 and AR048544). The authors are grateful to Drs. Katarzyna Gawron, Katarzyna Lazarz-Bartyzel, Mieczyslaw Lazarz, and Maria Chomyszyn-Gajewska (Jagiellonian University, Krakow, Poland) for generous gift of gingival fibroblasts. Moreover, the authors thank Anthony Kasinskas and Annie Ashok for help with biochemical and cell-based assays.

References

1. Beck A, Wurch T, Bailly C, Corvaia N. Strategies and challenges for the next generation of therapeutic antibodies. Nature reviews Immunology. 2010; 10:345–352.
2. Chadd HE, Chamow SM. Therapeutic antibody expression technology. Curr Opin Biotechnol. 2001; 12:188–194. [PubMed: 11287236]
3. Cheng JD, Rieger PT, von Mehren M, Adams GP, Weiner LM. Recent advances in immunotherapy and monoclonal antibody treatment of cancer. Semin Oncol Nurs. 2000; 16:2–12. [PubMed: 11151455]
4. Holliger P, Hudson PJ. Engineered antibody fragments and the rise of single domains. Nat Biotechnol. 2005; 23:1126–1136. [PubMed: 16151406]
5. Kim SJ, Park Y, Hong HJ. Antibody engineering for the development of therapeutic antibodies. Molecules and cells. 2005; 20:17–29. [PubMed: 16258237]
6. Nelson AL, Reichert JM. Development trends for therapeutic antibody fragments. Nat Biotechnol. 2009; 27:331–337. [PubMed: 19352366]
7. Chung HJ, Steplewski A, Chung KY, Uitto J, Fertala A. Collagen fibril formation. A new target to limit fibrosis. J Biol Chem. 2008; 283:25879–25886. [PubMed: 18650436]
8. Tucker PW, Slightom JL, Blattner FR. Mouse IgA heavy chain gene sequence: implications for evolution of immunoglobulin hinge axons. Proc Natl Acad Sci U S A. 1981; 78:7684–7688. [PubMed: 6801659]
9. Whitmore L, Wallace BA. DICHROWEB, an online server for protein secondary structure analyses from circular dichroism spectroscopic data. Nucleic Acids Res. 2004; 32:W668–673. [PubMed: 15215473]
10. Akesson P, Moritz L, Truedsson M, Christensson B, von Pawel-Rammingen U. IdeS, a highly specific immunoglobulin G (IgG)-cleaving enzyme from Streptococcus pyogenes, is inhibited by specific IgG antibodies generated during infection. Infect Immun. 2006; 74:497–503. [PubMed: 16369006]
11. Vincents B, von Pawel-Rammingen U, Bjorck L, Abrahamson M. Enzymatic characterization of the streptococcal endopeptidase, IdeS, reveals that it is a cysteine protease with strict specificity for IgG cleavage due to exosite binding. Biochemistry. 2004; 43:15540–15549. [PubMed: 15581366]
12. Brittingham R, Uitto J, Fertala A. High-affinity binding of the NC1 domain of collagen VII to laminin 5 and collagen IV. Biochem Biophys Res Commun. 2006; 343:692–699. [PubMed: 16563355]
13. Sieron AL, Louneva N, Fertala A. Site-specific interaction of bone morphogenetic protein 2 with procollagen ii. Cytokine. 2002; 18:214–221. [PubMed: 12126644]
14. Myszka DG, Morton TA. CLAMP: a biosensor kinetic data analysis program. Trends Biochem Sci. 1998; 23:149–150. [PubMed: 9584619]
15. Wang XQ, Liu YK, Qing C, Lu SL. A review of the effectiveness of antimitotic drug injections for hypertrophic scars and keloids. Ann Plast Surg. 2009; 63:688–692. [PubMed: 19887927]
16. Shin SJ, Lee SY. Efficacies of corticosteroid injection at different sites of the shoulder for the treatment of adhesive capsulitis. Journal of shoulder and elbow surgery/American Shoulder and Elbow Surgeons [et al]. 2012
17. Hsu JE, Anakwenze OA, Warrender WJ, Abboud JA. Current review of adhesive capsulitis. Journal of shoulder and elbow surgery/American Shoulder and Elbow Surgeons [et al]. 2011; 20:502–514.
18. Gaujoux-Viala C, Dougados M, Gossec L. Efficacy and safety of steroid injections for shoulder and elbow tendonitis: a meta-analysis of randomised controlled trials. Ann Rheum Dis. 2009; 68:1843–1849. [PubMed: 19054817]
19. Steplewski A, Fertala A. Inhibition of collagen fibril formation. Fibrogenesis Tissue Repair. 2012; 5(Suppl 1):S29. [PubMed: 23259659]
20. Prockop DJ, Fertala A. Inhibition of the self-assembly of collagen I into fibrils with synthetic peptides. Demonstration that assembly is driven by specific binding sites on the monomers. J Biol Chem. 1998; 273:15598–15604. [PubMed: 9624151]

21. Prockop DJ, Fertala A. The collagen fibril: the almost crystalline structure. Journal of structural biology. 1998; 122:111–118. [PubMed: 9724611]

22. Lobo ED, Hansen RJ, Balthasar JP. Antibody pharmacokinetics and pharmacodynamics. J Pharm Sci. 2004; 93:2645–2668. [PubMed: 15389672]

23. Dubel, S. Handbook of Therapeutic Antibodies. 1. Weinheim: Wiley-VCH Verlag GmbH&Co. KGaA; 2007.

24. Wang W, Wang EQ, Balthasar JP. Monoclonal antibody pharmacokinetics and pharmacodynamics. Clinical pharmacology and therapeutics. 2008; 84:548–558. [PubMed: 18784655]

25. Jenkins N, Murphy L, Tyther R. Post-translational modifications of recombinant proteins: significance for biopharmaceuticals. Mol Biotechnol. 2008; 39:113–118. [PubMed: 18327554]

26. Rosenberg AS. Effects of protein aggregates: an immunologic perspective. Aaps J. 2006; 8:E501–507. [PubMed: 17025268]

27. Brych SR, Gokarn YR, Hultgen H, Stevenson RJ, Rajan R, Matsumura M. Characterization of antibody aggregation: role of buried, unpaired cysteines in particle formation. J Pharm Sci. 2010; 99:764–781. [PubMed: 19691118]

28. Canty EG, Lu Y, Meadows RS, Shaw MK, Holmes DF, Kadler KE. Coalignment of plasma membrane channels and protrusions (fibripositors) specifies the parallelism of tendon. J Cell Biol. 2004; 165:553–563. [PubMed: 15159420]

29. Holmes DF, Gilpin CJ, Baldock C, Ziese U, Koster AJ, Kadler KE. Corneal collagen fibril structure in three dimensions: Structural insights into fibril assembly, mechanical properties, and tissue organization. Proc Natl Acad Sci U S A. 2001; 98:7307–7312. [PubMed: 11390960]

30. Malone JP, Veis A. Heterotrimeric type I collagen C-telopeptide conformation as docked to its helix receptor. Biochemistry. 2004; 43:15358–15366. [PubMed: 15581348]

31. Antipova O, Orgel JP. Non-enzymatic decomposition of collagen fibers by a biglycan antibody and a plausible mechanism for rheumatoid arthritis. PLoS One. 2012; 7:e32241. [PubMed: 22427827]

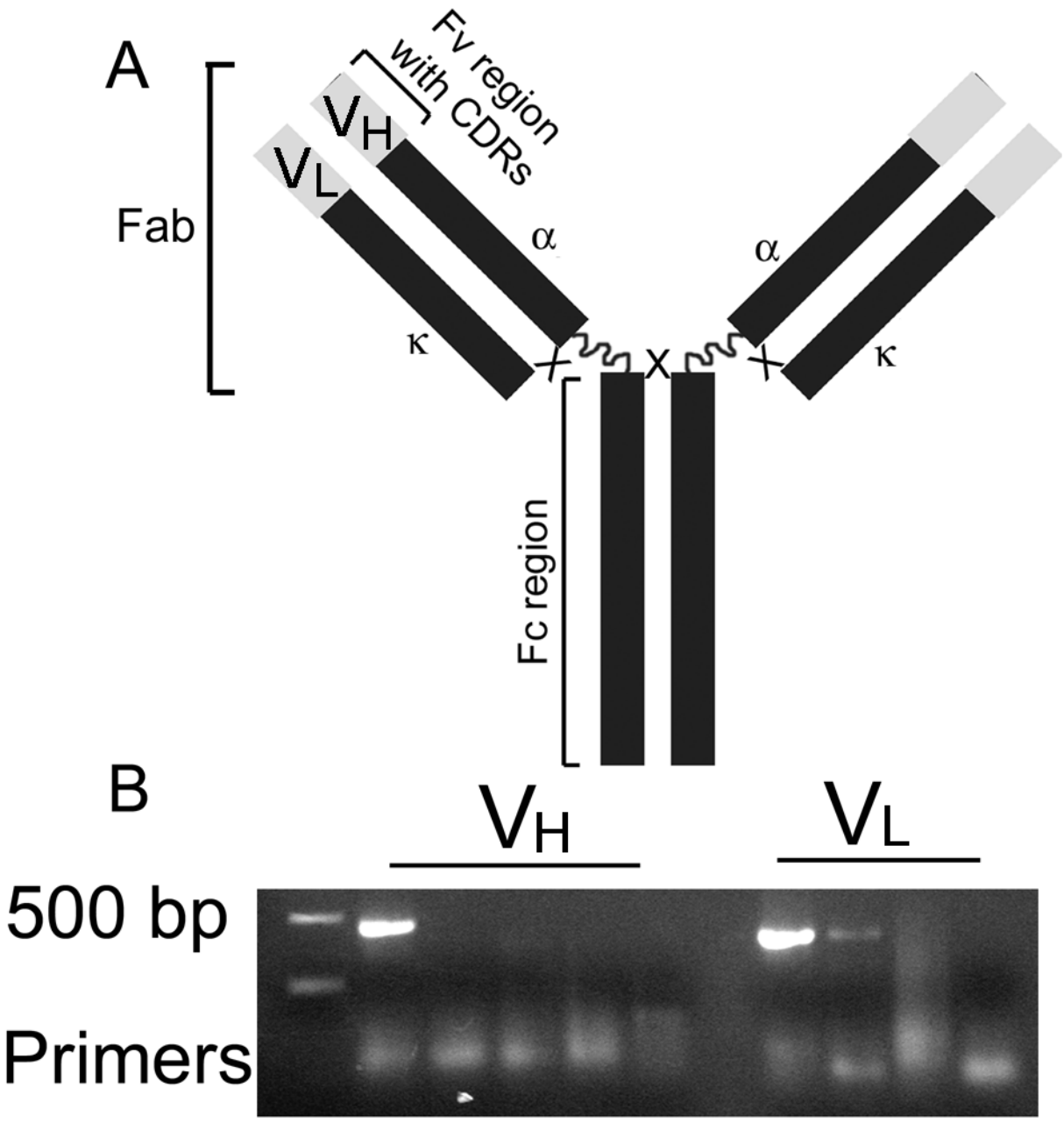

Figure 1.
PCR products corresponding to the variable regions of the ^{m}IgA-type anti-α2Ct antibody. A; A schematic illustrating relevant domains of the ^{m}IgA variant. B; PCR products encompassing DNA sequences that encode the variable regions of the heavy α (V_H) and the light κ (V_L) chains of the ^{m}IgA-type anti-α2Ct antibody. Note: Some sets of the PCR primers did not create any products due to the lack of homology with the variable regions of the template. Symbols: Fv; Fragment variable regions, CDR; Complementarity determining regions, α and κ; constant regions of the heavy α and light κ chains, respectively, Fab; Fragment antigen-binding, Fc; Fragment crystallizable region, Vα and Vκ; PCR products corresponding to the Fv regions of the α and κ chains, respectively.

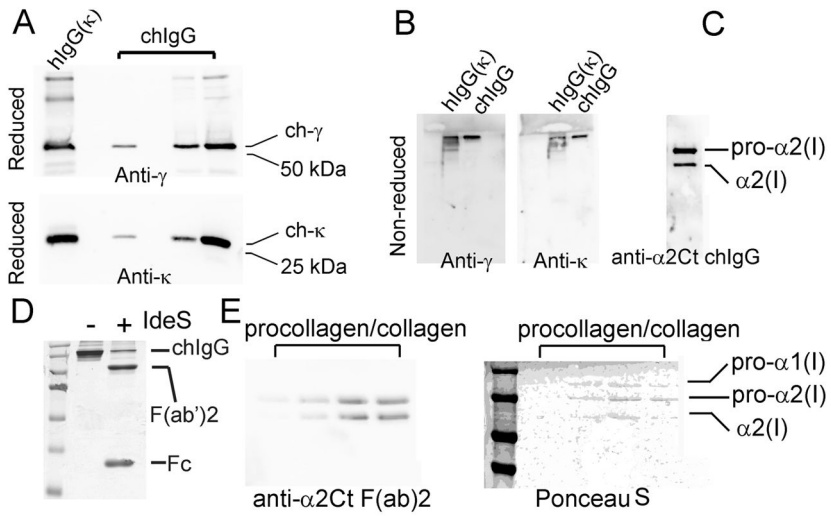

Figure 2.

Assays of the ^{ch}IgG variant of the anti-α2Ct antibody and its F(ab′)$_2$ fragment. A; Purified ^{ch}IgG variant produced by CHO cells was analyzed in reducing conditions for the presence of the γ (upper panel) and κ chains (lower panel). Specific antibodies against particular chains confirm the production of the γ and κ chains by CHO cells, B; Purified ^{ch}IgG variant was analyzed in non-reducing conditions for the ability of the γ and κ chains to assemble into disulfide bonded molecules. The presence of the high molecular band, detected with both the anti-γ and the anti-κ antibodies, indicates correct folding of the ^{ch}IgG molecules. The ^{h}IgG variant which contains the κ chain was used as a positive marker. C; Western blot assays of the specificity of the ^{ch}IgG variant for binding the α2Ct antigen. The two bands visible in the blot represent an intact and partially processed pro-α2 chain both specifically recognized by the ^{ch}IgG. D; Non-reducing electrophoretic separation of the intact ^{ch}IgG and its F(ab′)$_2$ and Fc fragments generated by the enzymatic cleavage with IdeS. E; Western blot assays (left panel) of the binding of the F(ab′)$_2$ fragment to the pro-α2 chain or its partially degraded form (a few different concentrations of procollagen I were applied onto separate lines). Corresponding staining of a nitrocellulose membrane with Ponceau S (right panel) identifies bands positively stained with the use of the F(ab′)$_2$ fragment of the ^{ch}IgG variant. Symbols: hIgG(k) and chIgG; control human IgG with the κ light chain and the ^{ch}IgG variant, respectively, ch-γ and ch-κ; chimeric γ and κ chains of the ^{ch}IgG, respectively, Anti-γ and Anti-κ; specific antibodies employed to detect the ch-γ and ch-κ chains of the ^{ch}IgG, anti-α2Ct chIgG; the chIgG variant tested for its ability to detect the α2Ct, Fab; Fragment antigen-binding, Fc; Fragment crystallizable region, anti-a2Ct F(ab)2; the F(ab′)$_2$ fragment of the ^{ch}IgG variant tested for its ability to detect the α2Ct Coomassie blue, Ponceau S; dyes employed to stain indicated samples, −/+ indicates the samples that were non-treated or treated with IdeS.

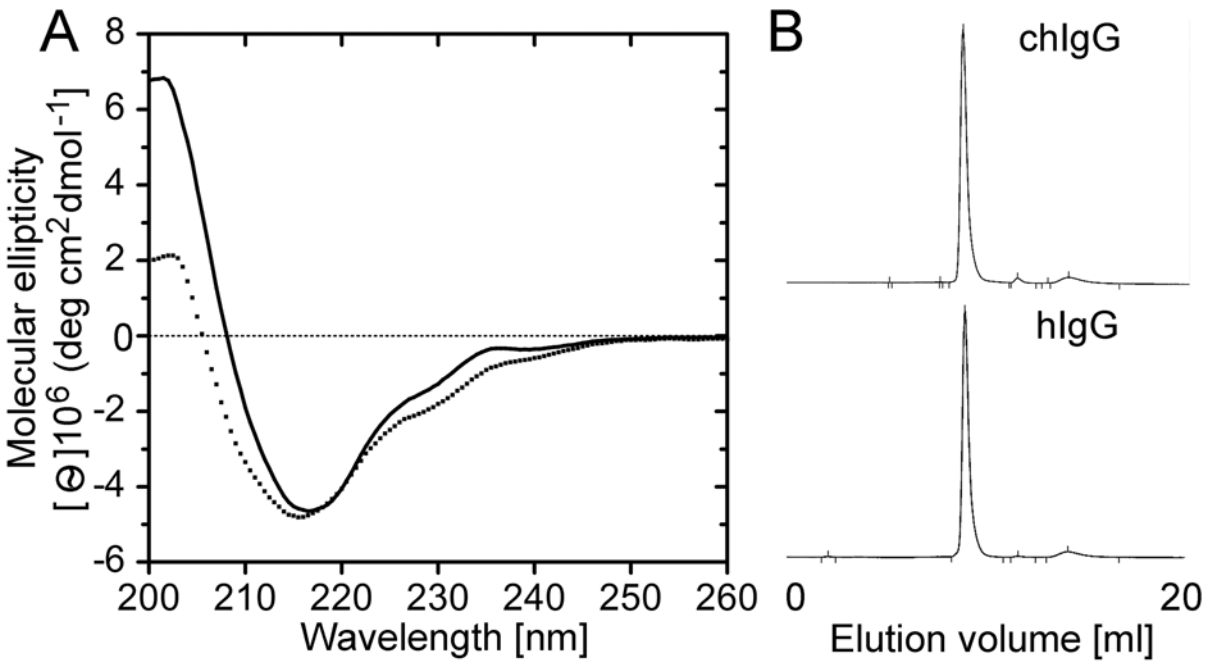

Figure 3.
Structural assays of the recombinant ^{ch}IgG variant. A; CD assays done on the ^{ch}IgG (dotted line) and ^{h}IgG control (solid line). B; Chromatography profiles illustrating elution characteristics of the analyzed IgG variants.

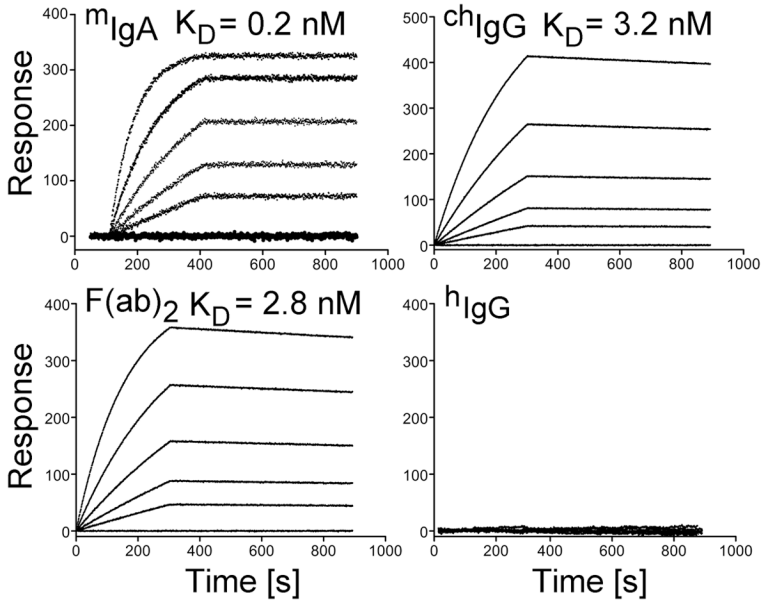

Figure 4.

Kinetics of the binding of the anti-α2Ct antibody variants to procollagen I. In each panel, the curves represent association and dissociation events during analyzed binding interactions between procollagen I and antibody variants present at concentrations ranging from 12.5 nM to 200 nM. For each assay, the association rate constants (k_{on}) and the dissociation rate constants (k_{off}) were obtained, and the equilibrium dissociation constants (K_D) values were calculated from a ratio of k_{off}/k_{on}.

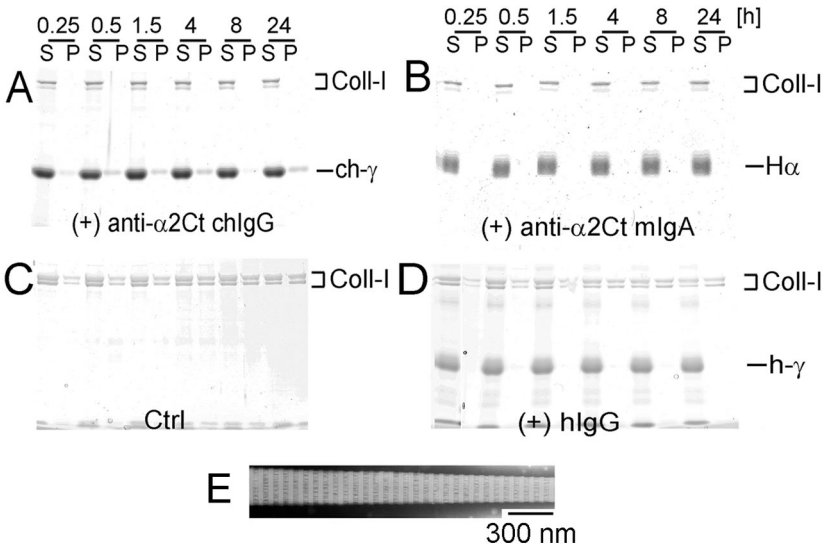

Figure 5.

Effects of the ^{ch}IgG on collagen fibril formation *in vitro*. Collagen fibrils were formed in the presence of tested antibodies added to collagen I in a 1:1 molar ratio. At the indicated points, collagen fibrils were separated from free collagen monomers by centrifugation. Subsequently pellet (fibrils) and supernatant (monomers) fractions were analyzed by gel electrophoresis. A and B: Experimental groups in which collagen fibrils were formed in the presence of the ^{ch}IgG or the ^{m}IgA variants of the anti-α2-Ct antibody,, respectively. C and D; Control groups in which collagen fibrils were formed in the absence of antibodies or in the presence of non-inhibitory ^{h}IgG, respectively. E; EM images of representative fibrils formed in a control group. Symbols: P and S; pellet and supernatant fractions, respectively, α, h-γ, and ch-γ; heavy α chain of the ^{m}IgA variant, heavy γ chain of the ^{h}IgG variant, and heavy γ chain of the ^{ch}IgG, Coll-I; α1 and α2 chains of collagen I.

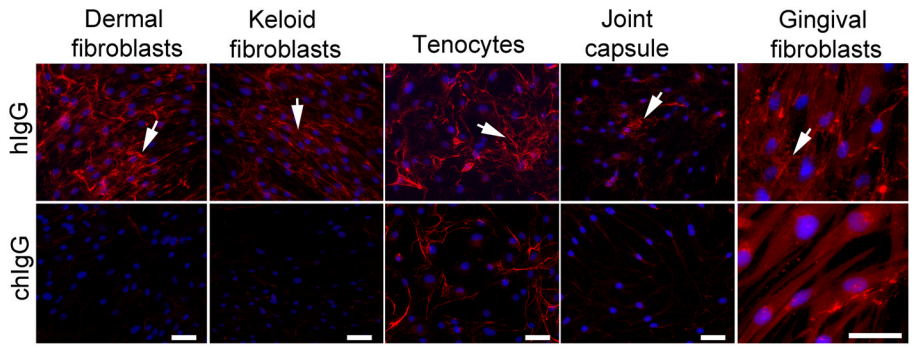

Figure 6.

Microscopic assays of collagen fibrils deposited in layers of cells cultured in the presence of control ^{h}IgG (upper row) or the inhibitory ^{ch}IgG variant of the anti-α2Ct antibody (bottom row). Because collagen fibrils produced by gingival fibroblasts isolated from a patient with the idiopathic form of gingival fibromatosis appear as thin filaments, larger images are presented to visualize them. Arrows indicate extracellular collagen deposits. Bars = 50 μm.

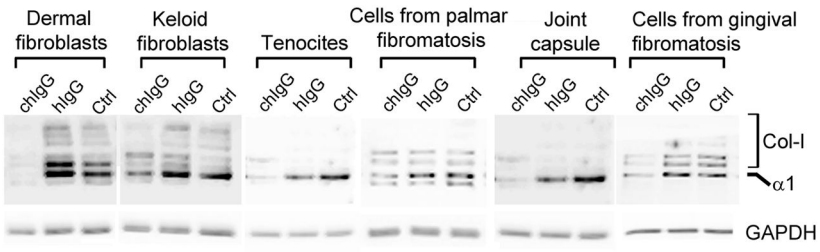

Figure 7.

Western blot assays of collagen I extracted from cell layers similar to those seen in Fig. 6. Note that in the presence of the inhibitory ^{ch}IgG, the amount of deposited collagen I is reduced in all analyzed cell lines. Symbols: chIgG, inhibitory ^{ch}IgG variant; hIgG, control non-inhibitory ^{h}IgG; Ctrl, samples not treated with any of the IgG variants, Col-I partially processed pro-α1 chains and cross-linked forms of α1 chains, GAPDH; glyceraldehyde 3-phosphate dehydrogenase; indicates uniform gel loading and provides a reference for the α1 collagen chain.

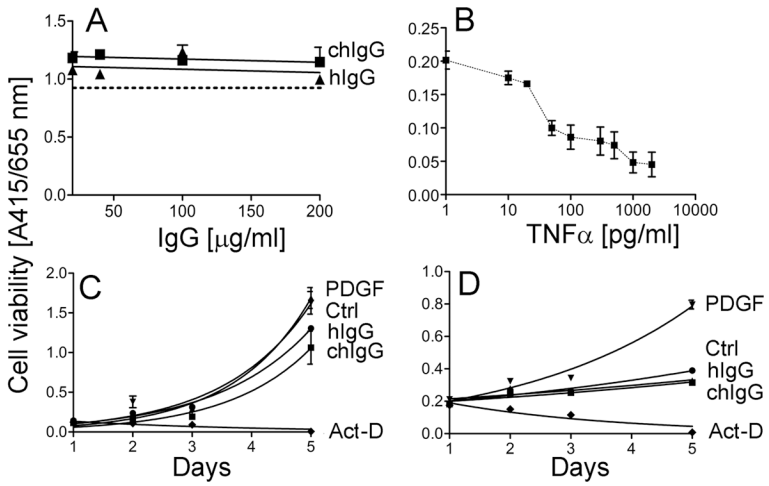

Figure 8.

Analysis of the effects of the ^{ch}IgG variant on the viability of cells. A; Assays of the viability of dermal fibroblasts as the function of a 24-h treatment with increasing concentrations of the ^{ch}IgG variant or control ^{h}IgG. The dotted line represents data for cells cultured in the absence of antibodies. B; The ability of WST-8-based assays to detect changes in the viability of fibroblastic cells was monitored in dermal fibroblasts cultured in the presence of various concentrations of TNFα. C and D; Proliferation assays of dermal fibroblasts (C) and cells isolated from the tendon sheaths (D) cultured in the presence of 100 μg/ml of tested antibodies. In addition, proliferation of cells cultured in the presence of PDGF or actinomycin D (Act-D) was also monitored. Moreover, a control (Ctrl) group of cells cultured in the absence of tested agents was also analyzed.

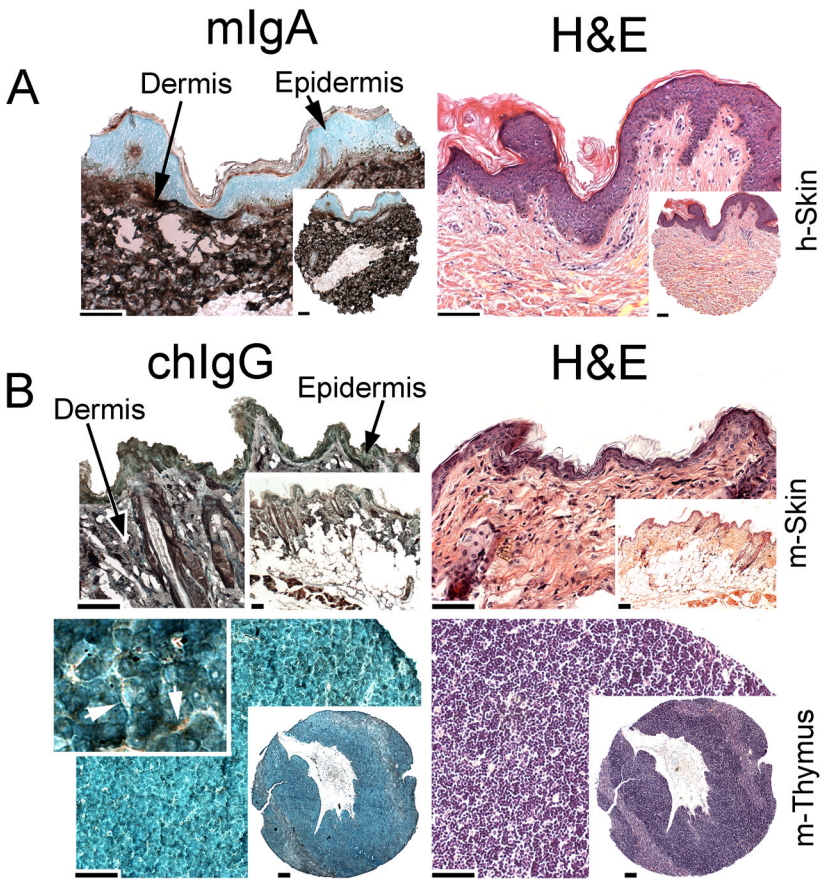

Figure 9.

Cross-reactivity assays of the ^{m}IgA and ^{ch}IgG variants of the anti-α2Ct antibody. The human skin sample (A) was immunostained with the ^{m}IgA variant, while the mouse skin and thymus were immunostained with the ^{ch}IgG form of the anti-α2Ct antibody (B). Corresponding panels were stained with H&E. As depicted in panel A, staining of the human skin (h-Skin) has revealed that collagen I -specific staining was limited to the collagen-rich dermis while the epidermis was collagen I-negative. Panel B demonstrates collagen I-positive staining of the dermal layer of the mouse skin (m-Skin), whereas the epidermis is collagen I-negative. In the mouse thymus (m-Thymus), collagen I-positive staining is apparent only in the interlobular regions (arrows). Bars = 50 μm.

Table I

Sets of primers employed to generate PCR products spanning the sequence encoding the V_H of the heavy α chain of the mouse IgA.

[a] Sets of forward PCR primers targeting the 5′ end of the sequence encoding the V_H of the mouse heavy μ chain (Ig-Primer Set EMD Millipore/Novagen)	[b] Reverse PCR primers targeting the 5′ end of the sequence encoding the constant region of the mouse heavy α chain [a]
$MuIg_H5'$-A	α1_1 GGGAGTGTCAGTGGGTAGATGGTG*
$MuIg_H5'$-B	α1_2 TTCCCACTCTTTCCCCAGGTCACA
$MuIg_H5'$-C*	α1_3 AGAGGCGAGGGCAGGTGGAAAGTT
$MuIg_H5'$-D	α1_4 CAGAGGCGAGGGCAGGTGGAAAGT
$MuIg_H5'$-E	α1_5 TCACGGATCTCCTTCTGGGCACTG
$MuIg_H5'$-F	

[a] Detailed information on these primers can be found in the manual for the Ig-Primer Set (EMD Millipore/Novagen).

[b] Primers were designed based on the DNA sequence of the mouse IgA heavy α chain published by Tucker *et al*. [8].

* A primer set that resulted in a PCR product encompassing the V_H region of the α chain of mouse IgA (see Fig. 1).